

## Segmented Spiral Waves and Anti-phase Synchronization in a Model System with Two Identical Time-Delayed Coupled Layers\*

YUAN Guo-Yong,<sup>1,†</sup> YANG Shi-Ping,<sup>1</sup> WANG Guang-Rui,<sup>2</sup> and CHEN Shi-Gang<sup>2</sup>

<sup>1</sup>Department of Physics, Hebei Normal University, Shijiazhuang 050016, China

<sup>2</sup>Institute of Applied Physics and Computational Mathematics, P.O. Box 8009, Beijing 100088, China

(Received January 24, 2007; Revised March 6, 2007)

**Abstract** In this paper, we consider a model system with two identical time-delayed coupled layers. Synchronization and anti-phase synchronization are exhibited in the reactive system without diffusion term. New segmented spiral waves, which are constituted by many thin trips, are found in each layer of two identical time-delayed coupled layers, and are different from the segmented spiral waves in a water-in-oil aerosol sodium bis(2-ethylhexyl) sulfosuccinate (AOT) micro-emulsion (ME) (BZ-AOT system), which consists of many small segments. “Anti-phase spiral wave synchronization” can be realized between the first layer and the second one. For different excitable parameters, we also give the minimum values of the coupling strength to generate segmented spiral waves and the tip orbits of spiral waves in the whole bilayer.

**PACS numbers:** 05.70.Ln, 05.45.Gg

**Key words:** spiral wave, synchronization, anti-phase synchronization

### 1 Introduction

Spiral waves are ubiquitous in various biological, chemical, and physical systems, such as cardiac muscle, the oxidation of CO on platinum, and the Belousov–Zhabotinsky (BZ) reaction.<sup>[1]</sup> Spiral waves are a kind of beautiful and significant patterns in nature, and are broadly studied, for example, the motion of the tip and the control of spiral waves.<sup>[2–7]</sup> Further study of spiral waves has revealed the existence of more phenomena, multiarmed,<sup>[8]</sup> super-,<sup>[9]</sup> ripple,<sup>[10]</sup> zigzag-,<sup>[11]</sup> and inwardly propagating (anti-) spirals<sup>[12]</sup> have successively been found. Recently it has been the fact that the spiral and concentric (target) waves are always not smooth and continuous: The formation of a period-doubled spiral waveform with broken rotational symmetry is investigated in oscillatory media exhibiting period-doubling bifurcations; The experiment of the BZ reaction in a water-in-oil aerosol sodium bis(2-ethylhexyl) sulfosuccinate (AOT) micro-emulsion (ME) (BZ-AOT) system exhibits also the segmented spiral waves.<sup>[13]</sup>

In this paper, a model system with two identical time-delayed coupled layers is considered. The model is practical, and can be used to simulate many real systems, for example, two layers of intestine, two coupled neurons, cardiorespiratory system, and BZ systems. With the development of experiment technology and condition, two distributed BZ systems with local coupling are also experimentally investigated.<sup>[14]</sup> Coupled spatially extended systems have attracted increasing attention. As a result of our work, segmented spiral waves consisting of many

thin trips can be observed, and anti-phase spiral waves synchronization can happen in our considered model.

### 2 The Model

Each layer in the considered model is described by the FitzHugh–Nagumo (FHN) model,<sup>[15]</sup> which was derived to mimic Hodgkin–Huxley membrane dynamics while maintaining the simplicity and physical meaning of the famous Van der Pol oscillator. The FHN model was widely used to simulate the dynamics of biological systems, including microbial populations and heart. The term of time-delayed couple is applied in the FHN model of each layer, the studied bilayer can be described by the following equation:

$$\frac{\partial u_1}{\partial t} = \frac{1}{\varepsilon} [f(u_1, v_1) + c(u_2(t - \tau) - u_1(t - \tau))] + \nabla^2 u_1, \quad (1)$$

$$\frac{\partial v_1}{\partial t} = g(u_1, v_1), \quad (2)$$

$$\frac{\partial u_2}{\partial t} = \frac{1}{\varepsilon} [f(u_2, v_2) + c(u_1(t - \tau) - u_2(t - \tau))] + \nabla^2 u_2, \quad (3)$$

$$\frac{\partial v_2}{\partial t} = g(u_2, v_2), \quad (4)$$

where  $f(u, v) = -v - u(u - a)(u - 1)$  and  $g(u, v) = -\gamma v + \beta u - \delta$ . In the model,  $u$  and  $v$  describe separately membrane voltage (fast or activator variable) and  $v$ -gate (slow or inhibitor variable),  $a$  represents the threshold for excitation,  $\varepsilon$  represents the excitability and  $\beta$ ,  $\gamma$ , and  $\delta$  are parameters that can change the rest state and dynamics. By truncating a travel wave, a spiral wave can be formed in each layer without the coupling. Here, we consider the system consisting of two time-delay coupled layers, which are common in real systems, especially in biological sys-

\*The project supported by National Natural Science Foundation of China under Grant No. 10647127, National Natural Science Foundation of China for Major Projects under Grant No. 10335010, and the Natural Science Foundation of Hebei Province of China under Grant No. A2006000128

<sup>†</sup>E-mail: g-y-1975@sohu.com

tems, where bilayer membranes or multilayer are often found. Previously, we have also considered the dynamics of the model with a spiral state and a rest one.<sup>[16]</sup> Here the model with two spiral states, which has a phase difference with each other is considered for a certain domain in details, and segmented spiral waves, which are new and anti-phase synchronization satisfying a spiral wave can be found. We will also study the tip dynamics in the whole bilayer under different coupled intensity in details, and give the domain of segmented spiral waves.

### 3 Dynamical Behavior of Reactive System Without Diffusion Term

We consider firstly the dynamical behavior of the corresponding reactive system. Without the diffusion term,

at the same time, we take  $t' = 1/\varepsilon t$ ,  $r = \gamma \times \varepsilon$ ,  $b = \beta \times \varepsilon$ , the following equation is obtained:

$$\begin{aligned} \frac{\partial u_1}{\partial t'} &= -v_1 - u_1^3 + (a+1)u_1^2 - au_1 \\ &\quad + c(u_2(t' - \tau') - u_1(t' - \tau')), \end{aligned} \quad (5)$$

$$\frac{\partial v_1}{\partial t'} = -rv_1 + bu_1, \quad (6)$$

$$\begin{aligned} \frac{\partial u_2}{\partial t'} &= -v_2 - u_2^3 + (a+1)u_2^2 - au_2 \\ &\quad + c(u_1(t' - \tau') - u_2(t' - \tau')), \end{aligned} \quad (7)$$

$$\frac{\partial v_2}{\partial t'} = -rv_2 + bu_2. \quad (8)$$

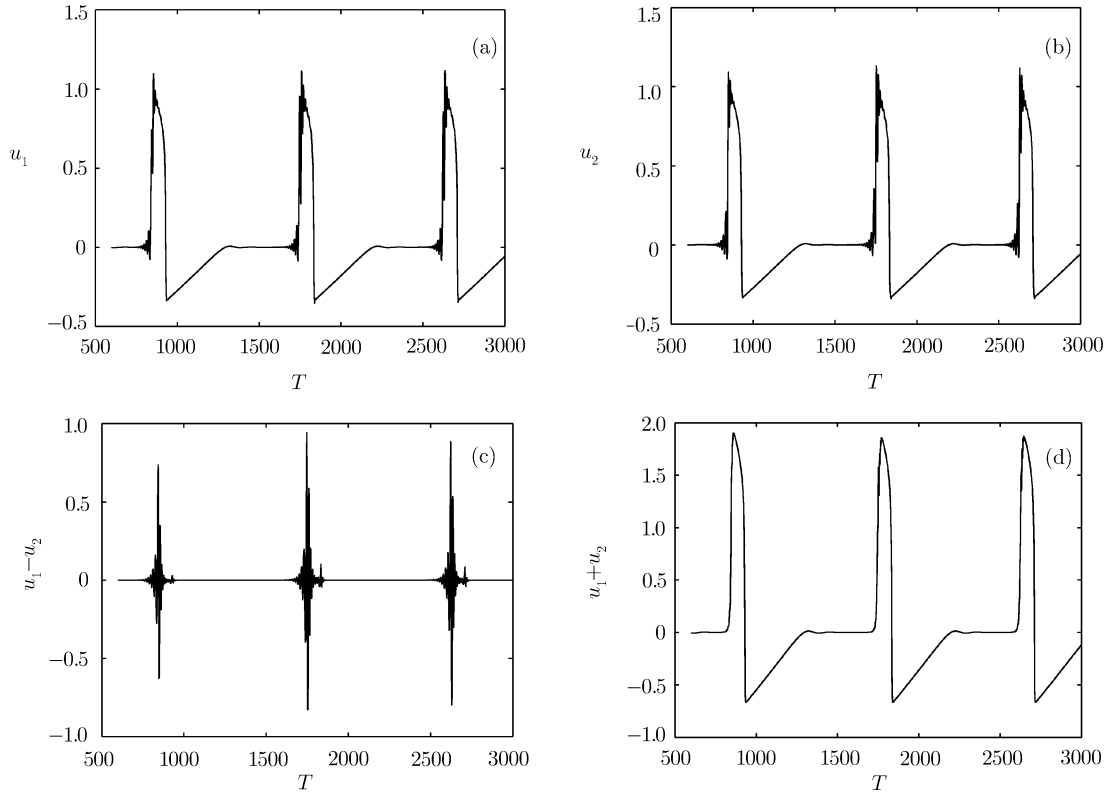


**Fig. 1** The time evolution of the activator variables in the reactive system without the diffusion term. (a)  $u_1$  vs. the number of time step  $n$ ; (b)  $u_2$  vs.  $n$ ; (c)  $u_1 - u_2$  vs.  $n$ ; (d)  $u_1 + u_2$  vs.  $n$ .

The point  $(u_1, v_1, u_2, v_2) = (0, 0, 0, 0)$  is the stationary solution of the equation, but its stability depends on  $\tau'$ . The characteristic equation of the whole reactive system is

$$\Delta_1(\lambda)\Delta_2(\lambda) = 0, \quad (9)$$

where

$$\Delta_1(\lambda) = [(a + \lambda)(r + \lambda) + b + 2.0ce^{-\lambda\tau'}(r + \lambda)], \quad (10)$$

$$\Delta_2(\lambda) = [(a + \lambda)(r + \lambda) + b]. \quad (11)$$

Let us first answer the question of local stability of the stationary point for all time-lags. In complex analysis, if complex-valued function  $f(z)$  is meromorphic in a region  $R$  enclosed by a contour  $C$ , let  $N$  be the number of complex roots of  $f(z)$  in  $C$ , and  $P$  be the number of poles in  $C$ , with each zero and pole counted as many times as its multiplicity and order, respectively. Then  $N - P = (1/2\pi i) \int_C [f'(z)/f(z)] dz$ . Defining  $w \equiv f(z)$  and  $\sigma \equiv f(C)$  gives  $N - P = (1/2\pi i) \int_\sigma (1/w) dw$ , the

above contents are called as argument principle. On the basis of argument principle, Rouch's theorem can be derived. Rouch's theorem tells us that if the complex-valued function  $f(z)$  and  $g(z)$  are holomorphic inside and on some closed contour  $C$ , with  $|g(z)| < |f(z)|$  on the  $C$ , then  $f(z)$  and  $f(z) + g(z)$  have the same number of zeros inside  $C$ , where each zero is counted as many times as its multiplicity. This theorem assumes that the contour  $C$  is simple, that is, without self-intersections, and it is oriented counter-clockwise. Due to Rouch's theorem, the existence and the number of roots about complex equations can easily be known by the existence and the number of roots about simple equations. According to argument principle and Rouch's theorem, we have proved that the stationary point remains locally stable for all time-lags if the coupling constant is below some value  $c^{\tau'}$ , which is given by

$$c^{\tau'} = \sqrt{\frac{a^2 r^2 - 2b + 2\sqrt{b(2r^2 + 2ar + b^2)}}{4}}. \quad (12)$$

The previous expression for  $c^{\tau'}$  is valid if  $b > r^2$  and  $4(b/r) > (a-1)^2$ , which is always satisfied in our model. When  $c > c^{\tau'}$ , local stability of the stationary depends on  $\tau'$ . More details are obtained by the analysis of the bifurcation. We can get the corresponding critical time lag, if

$$\sin(\omega\tau') = \frac{\omega_{\pm}^3 - (b-r^2)\omega_{\pm}}{2c(\omega_{\pm}^2 + r^2)} > 0, \quad (13)$$

then

$$\tau'_{1,\pm}{}^j = \frac{1}{\omega_{\pm}} \left[ 2j\pi + \cos^{-1} \left( \frac{-a\omega_{\pm}^2 - (ar+b)r}{2c(\omega_{\pm}^2 + r^2)} \right) \right], \quad j = 0, 1, 2, \dots, \quad (14)$$

and if

$$\sin(\omega\tau') = \frac{\omega_{\pm}^3 - (b-r^2)\omega_{\pm}}{2c(\omega_{\pm}^2 + r^2)} < 0, \quad (15)$$

then

$$\tau'_{1,\pm}{}^j = \frac{1}{\omega_{\pm}} \left[ (2j+2)\pi - \cos^{-1} \left( \frac{-a\omega_{\pm}^2 - (ar+b)r}{2c(\omega_{\pm}^2 + r^2)} \right) \right], \quad j = 0, 1, 2, \dots, \quad (16)$$

where  $\omega_{\pm} = \sqrt{(-A \pm \sqrt{A^2 - 4B})/2}$ ,  $A = a^2 + r^2 - 2b - 4c^2$ ,  $B = (ar+b)^2 - 4c^2 r^2$ . The previous formulas give bifurcation curves in the plane  $(\tau', c)$  for fixed values of the parameters  $a$ ,  $b$ , and  $r$ . The bifurcations are either subcritical Hopf on the curves  $\tau'_{1,-}{}^j$  leading to a disappearance of one unstable plane, or supercritical Hopf on  $\tau'_{1,+}{}^j$  resulting in appearance of an unstable one. The point  $(\tau', c) = (4, 0.27)$ , which is used in the following, is above the curve  $\tau'_{1,+}{}^0$  and below the curve  $\tau'_{1,+}{}^1$ , and far below the curve  $\tau'_{1,-}{}^0$ , so the stationary solution is unstable.

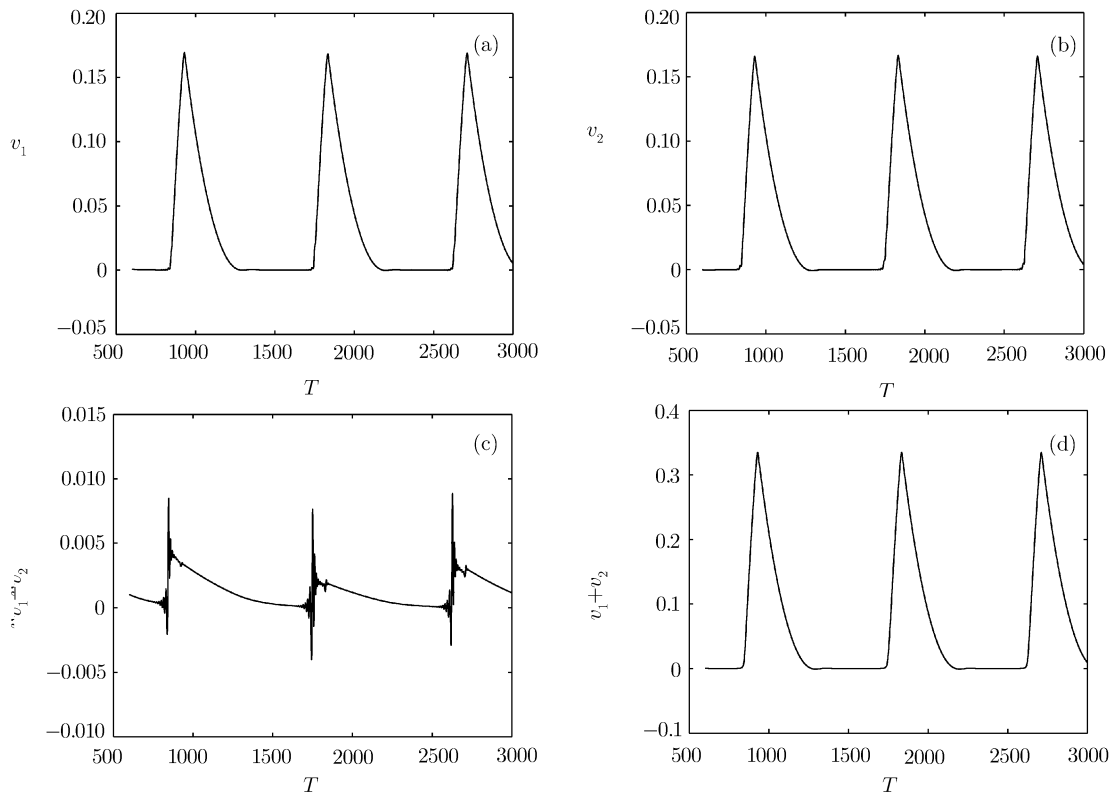


**Fig. 2** The time evolution of the inhibitor variables in the reactive system without the diffusion term. (a)  $v_1$  vs. the number of time step  $n$ ; (b)  $v_2$  vs.  $n$ ; (c)  $v_1 - v_2$  vs.  $n$  and (d)  $v_1 + v_2$  vs.  $n$ .

In the following, we consider the evolution of the whole reactive system with time, as shown in Figs. 1 and 2. The initial states of  $(u_1, v_1)$  and  $(u_2, v_2)$  correspond respectively to the excited and the recovery ones. Due to the instability of the stationary solution, the system cannot stay in the stationary state, but is continuously excited. It is easily seen from Fig. 1(d) that the anti-phase synchronization with certain condition and synchronization happen. In addition, the time development of  $(u_1 + u_2)$  and  $(v_1 + v_2)$  is smooth, and in one period, very similar to that of  $u$  and  $v$  in single FHN reactive system. These phenomena lead to complex behaviors in the corresponding spatially extended system together with diffusion effect. Figure 3 depicts their phases.

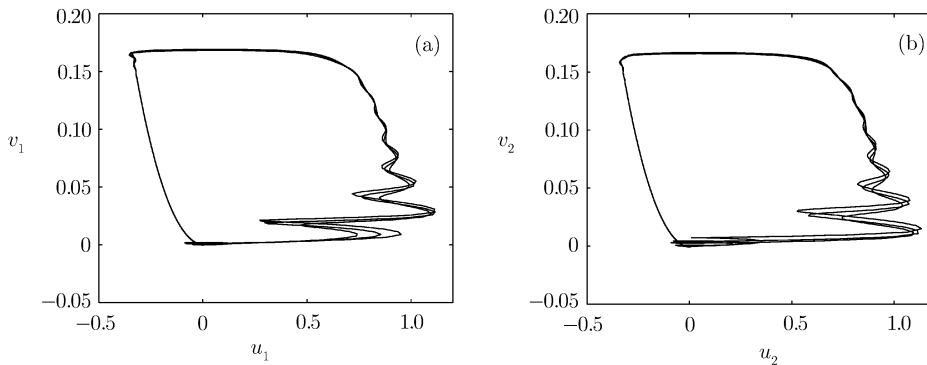


**Fig. 3** Phase chart in each layer of the bilayer. (a) In the first layer; (b) In the second layer.

#### 4 Segmented Spiral Wave and Anti-phase Spiral Wave Synchronization

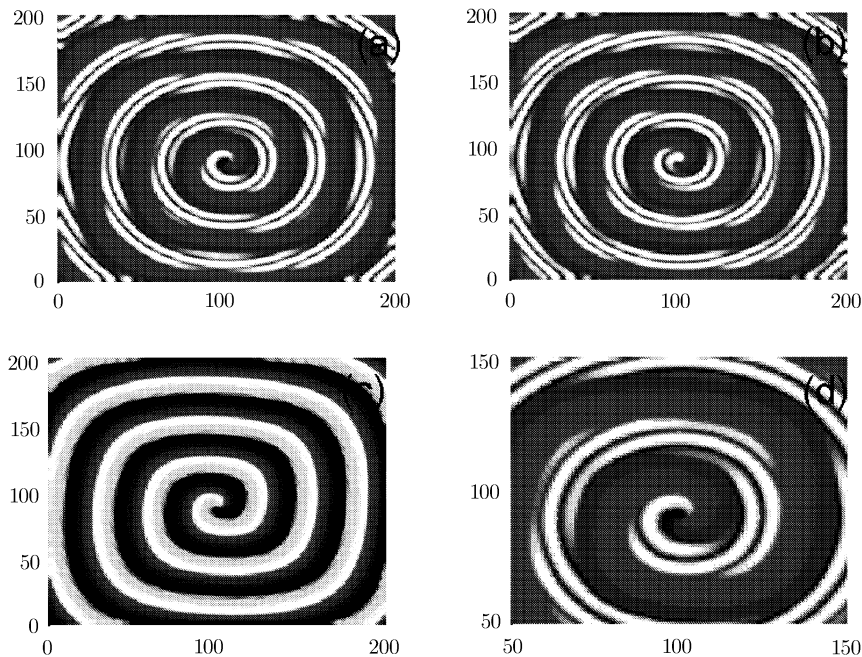


**Fig. 4** Segmented spiral waves consisting of many thin trips and “anti-phase spiral wave synchronization”. (a) The pattern in the first layer; (b) The pattern in the second layer; (c) A smooth spiral wave in the bilayer, which results from anti-phase wave spiral waves synchronization. (d) The enlarged pattern of (a).

The numeric experiment of the spatially extended system (depicted by Eqs. (1) ~ (4)) is undergone. In each layer, the number of space grids is  $200 \times 200$  and no-flux boundary is used. We take  $a = 0.03$ ,  $\delta = 0.0$ ,  $\beta = 2.5$ ,  $\gamma = -1.0$ ,  $c = 0.27$  and  $\varepsilon = 0.001$ . Two different evolutive states of the same spiral wave are respectively used as the initial states of the first layer and the second one in the bilayer system. After the transient adjustment, figure 4 can be very easy to be observed. It is surprising that each layer reveals segmented spiral waves, as shown in Figs. 4(a) and 4(b), which are different from the ones observed in the experiment of BZ-AOT. The former segmented spiral wave is consisting of many thin trips, while the later is formed by many small segments. In order to observe carefully and clearly the

segmented spiral wave in each layer, figure 4(a) is zoomed up and figure 4(d) is obtained.

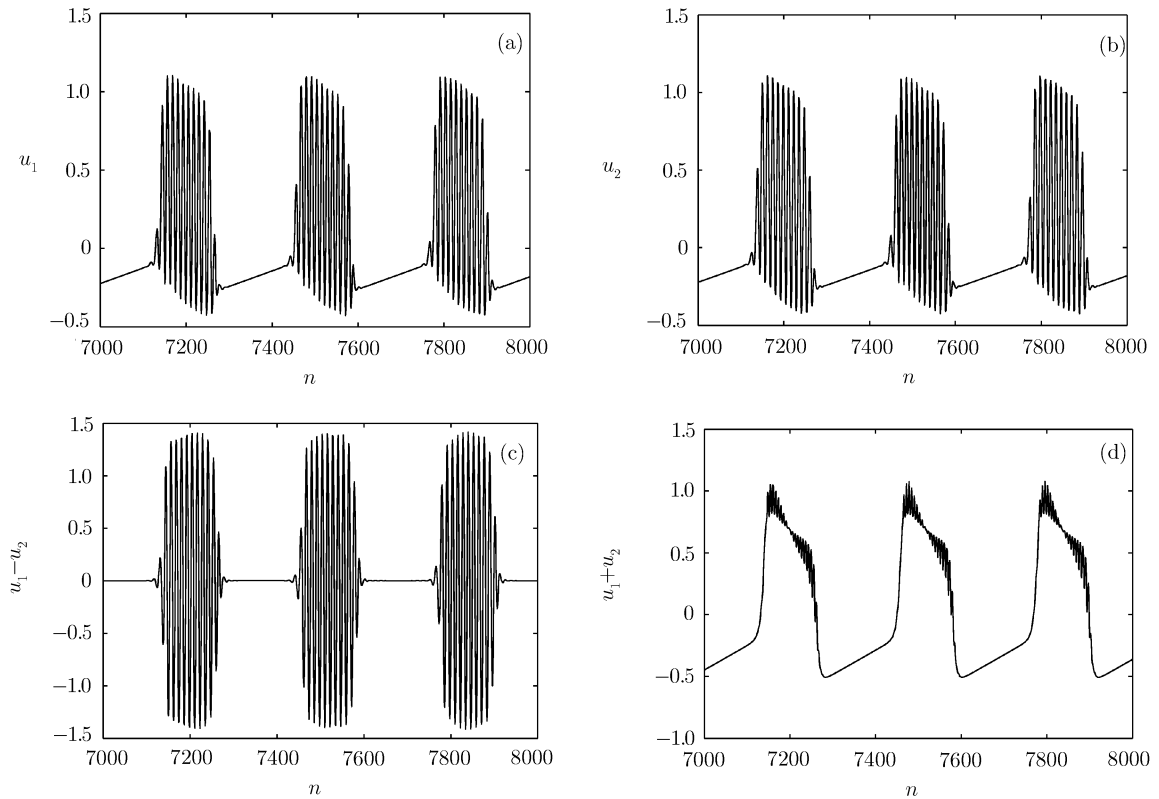


**Fig. 5** The time evolution of the activator variables on the point (150, 100) of the segmented spiral waves. (a)  $u_1$  vs. the number of time step  $n$ ; (b)  $u_2$  vs.  $n$ ; (c)  $u_1 - u_2$  vs.  $n$  and (d)  $u_1 + u_2$  vs.  $n$ .

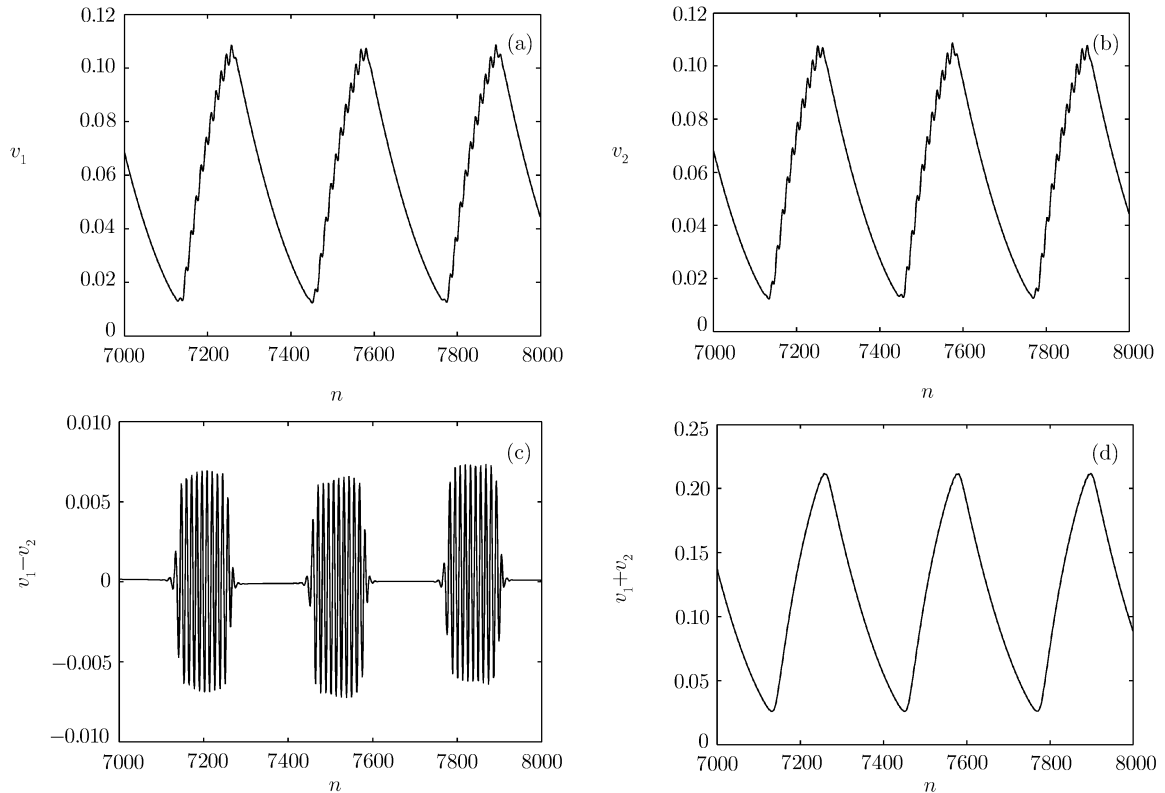


**Fig. 6** The time evolution of the inhibitor variables on the point (150, 100) of the segmented spiral waves. (a)  $v_1$  vs. the number of time step  $n$ ; (b)  $v_2$  vs.  $n$ ; (c)  $v_1 - v_2$  vs.  $n$ , and (d)  $v_1 + v_2$  vs.  $n$ .

The change of the variables  $u_1$ ,  $v_1$ ,  $u_2$ , and  $v_2$  with time  $t$  on the point (150,100) is recorded in Figs. 5 and 6. It is the fact that the recovery process on the point is smooth and steady, and accord with the recovery one on a certain point in each layer without the coupling, but the developmental process of the original excited state is asway and alternates between the state of  $u > 0.5$  and the one of  $u < 0.5$ , which is called as “oscillating excited states” by us. The steady recovery process between the first layer and the second one is synchronous, but the developmental one of oscillating excited state should be anti-phase synchronous, as shown in Figs. 5 and 6. It is easily seen that the state of the whole system ( $u_1 + u_2$ ) is a full spiral wave (shown in Fig. 4(c)), according to the concept of chaotic anti-phase synchronization, the phenomena are named as “anti-phase spiral wave synchronization”. Figures 5(d) and 6(d) reveal respectively the evolution of  $u_1 + u_2$  and  $v_1 + v_2$  with time, which agree with the ones of spiral wave in single FHN system. The tip trajectory of the spiral wave in the bilayer is unique, and different from spiral waves in single reactor-diffusion systems. The tip of the spiral wave moves along the petaline curve (Figs. 7(a) and 7(b)) in the single FHN system with the same parameter, while for the bilayer, the trajectory of the tip is coarsely astral (shown in Fig. 7(c)).

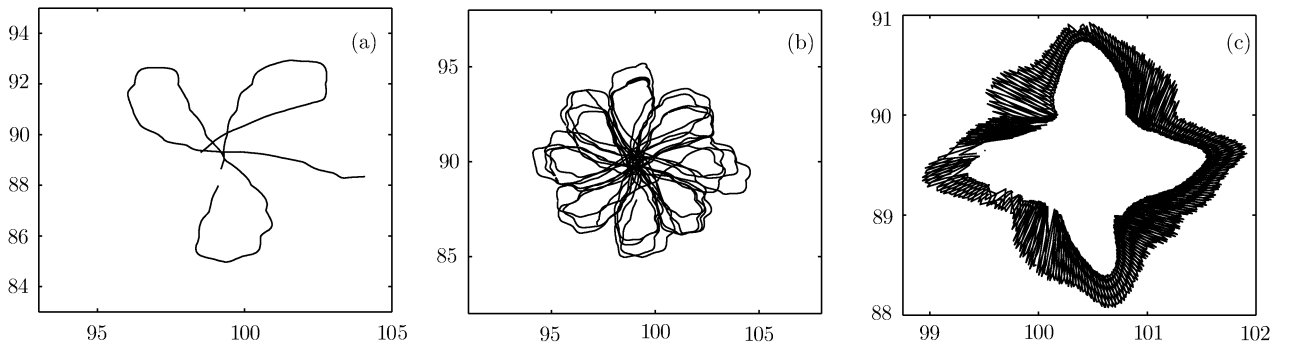


**Fig. 7** The motive trajectories of the tips. (a) and (b) depict the motion of spiral wave in single FHN model, which is petal-like; (b) Is a unit of (a). (c) Reveals the motion of smooth spiral waves in whole bilayer system, which is coarsely astral.

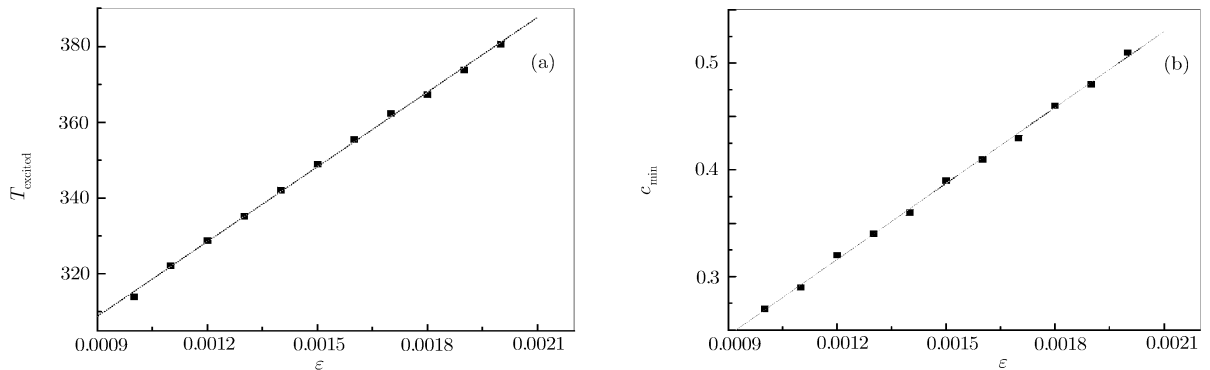


**Fig. 8** The excited periods  $T_{\text{excited}}$  and the minimum coupling parameters  $c_{\text{min}}$  to generate segmented spiral waves change with the excitable parameters  $\epsilon$ . (a)  $T_{\text{excited}}$  vs.  $\epsilon$ . (b)  $c_{\text{min}}$  vs.  $\epsilon$ . The numeric results are illustrated by dot. The lines show the results by linear fit.

Considering the behaviors under the different excitable parameter  $\epsilon$ , we find that the excited periods  $T_{\text{excited}}$  in a single layer without coupling (shown in Fig. 8(a)) and the minima of the coupling  $c_{\text{min}}$  to generate segmented spiral waves (shown in Fig. 8(b)) will nearly linearly increase with  $\epsilon$ . For a single layer with vanishing coupling intensity, with the increasing of  $\epsilon$ , the motive domain of tips will be enlarged. When  $\epsilon \leq 0.0037$ , the orbits are petal-like. When  $\epsilon \geq 0.0037$ , simple rotation spiral waves can exist in the system. Figure 9 depicts the motive trajectories of the tips for two different excitable parameters ( $\epsilon = 0.003$  and  $\epsilon = 0.0038$ ). The tips of spiral waves in the whole coupled bilayer move in the domains lesser than the motive ranges of tips in single layer without coupling. The shape of orbits in the whole bilayer approaches a circle when  $c$  is very large.

## 5 Conclusion and Discussion

In this paper, new segmented spiral waves are observed in each layer of the model system with two identical time-delayed coupled layers, which are built up by many nice trips, and are different from that in the experiment of BZ-AOT. “Anti-phase spiral wave synchronization” between two layers is named according to traditional anti-phase

synchronization relation between the chaotic systems. The phenomena contact with the dynamical nature of the corresponding reactive system without diffusion term, which represents two time-delayed coupled units. Bifurcational analyses of the system tell us that the stationary solution is instable due to supercritical Hopf, and that the system cannot stay finally in the stationary, and can be perpetually excited. The time evolution of the variables reveals the information related with the phenomena happening in the corresponding spatial extended system. It is true that there exist many complex patterns in nature, experiment, and numerical simulation, which is formed on the basis of the dynamics of the corresponding simple systems. We also discuss the tips in the whole bilayer and the minimum value of coupling intensity to generate a segmented spiral wave in a single layer.

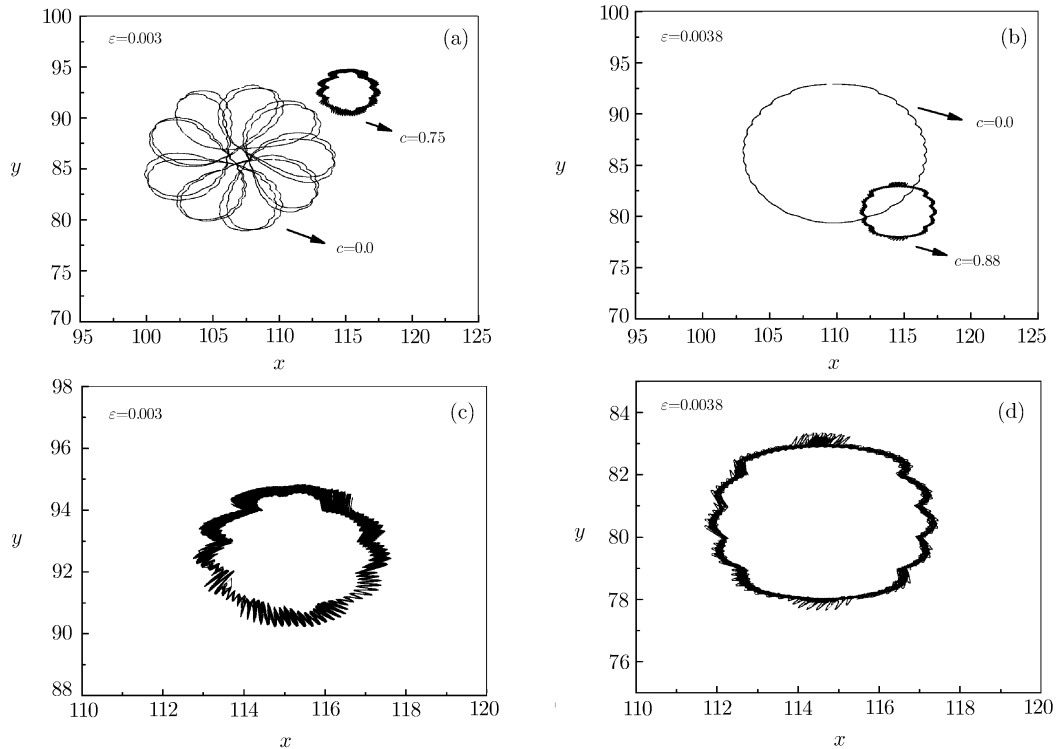


**Fig. 9** The motive trajectories of the tips for two different excitable parameters ( $\varepsilon = 0.003$  and  $\varepsilon = 0.0038$ ). (a) and (b) depict the motions of spiral wave in single FHN model with vanishing coupling intensity (indicated by  $c = 0.0$ ) and in the whole bilayer (signed by  $c = 0.75$  and  $c = 0.88$ ). (c), (d) show the enlargement of the drawing indicated by  $c = 0.75$  and  $c = 0.88$  in (a), (b).

## References

- [1] R. Kapral, and K. Showalter, *Chemical Waves and Patterns*, Kluwer, London (1995).
- [2] Sakaguchi Hidetsugu and Fujimoto Takefumi, *Phys. Rev. E* **67** (2003) 067202.
- [3] Woltering Matthias and Markus Mario, *Science Asia* **28** (2002) 43.
- [4] A.T. Stamp, G.V. Osopov, and J.J. Collins, *Chaos* **12** (2002) 931.
- [5] H. Zhang, B. Hu, and G. Hu, *Phys. Rev. E* **68** (2003) 026134.
- [6] Yuan Guo-Yong, Wang Guang-Rui, and Chen Shi-Gang, *Europhys. Lett.* **72** (2005) 908.
- [7] Ma Jun, Li Yan-Long, Jiang Jin-Long, Liu Yan-Jun, and Wang Chun-Ni, *Physica A* **369** (2006) 387.
- [8] K Agladze and V.I. Krinsky, *Nature (London)* **296** (1982) 424.
- [9] V. Perez-Munuzuri, R. Aliev, B. Vasiev, V. Perez-Villar, and V.I. Krinsky, *Nature (London)* **353** (1991) 740.
- [10] M Markus., G. Kloss, and I. Kusch, *Nature (London)* **371** (1994) 402.
- [11] Yu.A. Astrov, I. Muller, E. Ammelt, and H.G. Purwins, *Phys. Rev. Lett.* **80** (1998) 5341.
- [12] V.K. Vanag and I.R. Epstein, *Nature (London)* **294** (2001) 835.
- [13] V.K. Vanag and I.R Epstein, *PNAS* **100** (2003) 14635.
- [14] M . Hildebrand, J Cui, E. Mihaliuk, J. Wang, and K. Showalter, *Phys. Rev. E* **68** (2003) 026205.
- [15] R. FitzHugh, *et al.*, *Biophys. J.* **1** (1996) 445.
- [16] Yuan Guo-Yong, Yang Shi-Ping, Wang Guang-Rui, and Chen Shi-Gang, *Acta Phys. Sin.* **54** (2005) 1510 (in Chinese).